Electronic Supplementary Material (ESI) for CrystEngComm.

Aluminum Doping Effects on Photoresponse Characteristic of Hydrothermal Tin Disulfide Nanosheets

Xiancheng Meng, [a,c] *Chao Fan,*[a,b,c,*] *Xia An,*[a,c] *Shuo Yuan,*[a,c] *Yongkai Jing,*[a,c] *Zhe Liu,*[a,c] *Chun Sun,*[a,c] *Yonghui Zhang,*[a,c] *Zihui Zhang,*[a,c] *Mengjun Wang,*[a,b,c] *Hongxing Zheng* [a] *and Erping Li*[b]

a State Key Laboratory of Reliability and Intelligence of Electrical Equipment, Hebei University of Technology, Tianjin, 300401, China.

b Zhejiang Provincial Key Laboratory of Advanced Microelectronic Intelligent Systems and Applications, Hangzhou, 310027, China.

c Key Laboratory of Electronic Materials and Devices of Tianjin, Tianjin, 300401, China.

Corresponding Authors

* E-mail: fanch@hebut.edu.cn (C. Fan)

Content List

S-1 SEM images for the pristine and Al-doped SnS_2 nanosheets with different concentrations.

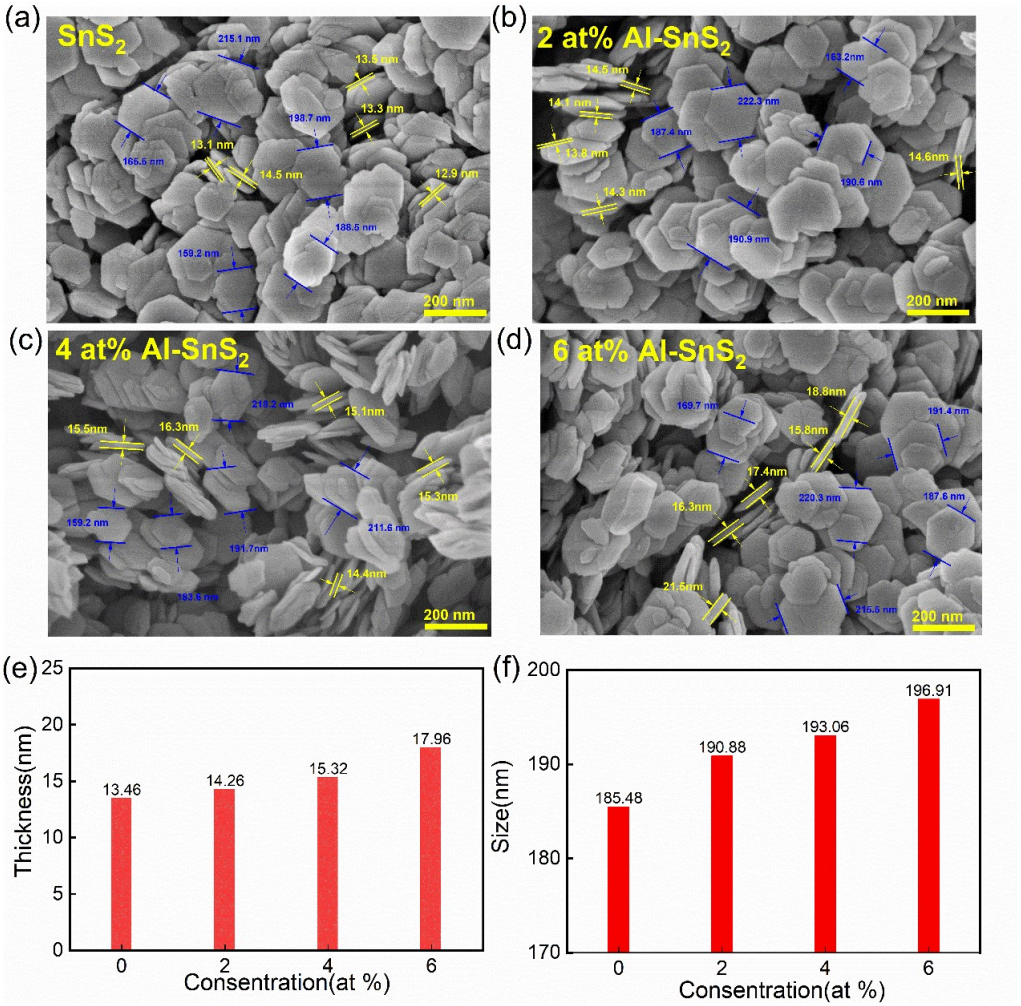

Figure S1. SEM images for the pristine and Al-doped SnS_2 nanosheets with different concentrations. SEM images of the (a) Pristine SnS_2, (b) 2 % Al-SnS_2, (c) 4 % Al-SnS_2, (d) 6 % Al-SnS_2 nanosheets. Statistical diagrams of the (e) thickness and (f) size for the pristine and Al-doped SnS_2 nanosheets.

Figures S1a and d shows SEM images for the pristine and Al-doped SnS_2 nanosheets with different Al concentrations. Figures S1c and d shows statistical data of the thickness and size for the pristine and Al-doped SnS_2 nanosheets. The thickness and size are 13.46 and 185.48 nm for the pristine SnS_2 nanosheets, 14.26 and 190.88 nm for the 2 at% Al-doped SnS_2 nanosheets, 15.32 and 193.06 nm for the 4 at% Al-doped SnS_2 nanosheets, 17.96 and 196.91 nm for the 6 at% Al-doped SnS_2 nanosheets. The thickness and size of nanosheets tends to increase gradually.

S-2 Photoresponse characterization for the pristine and Al-doped SnS_2 nanosheets under illumination of a 532-nm laser.

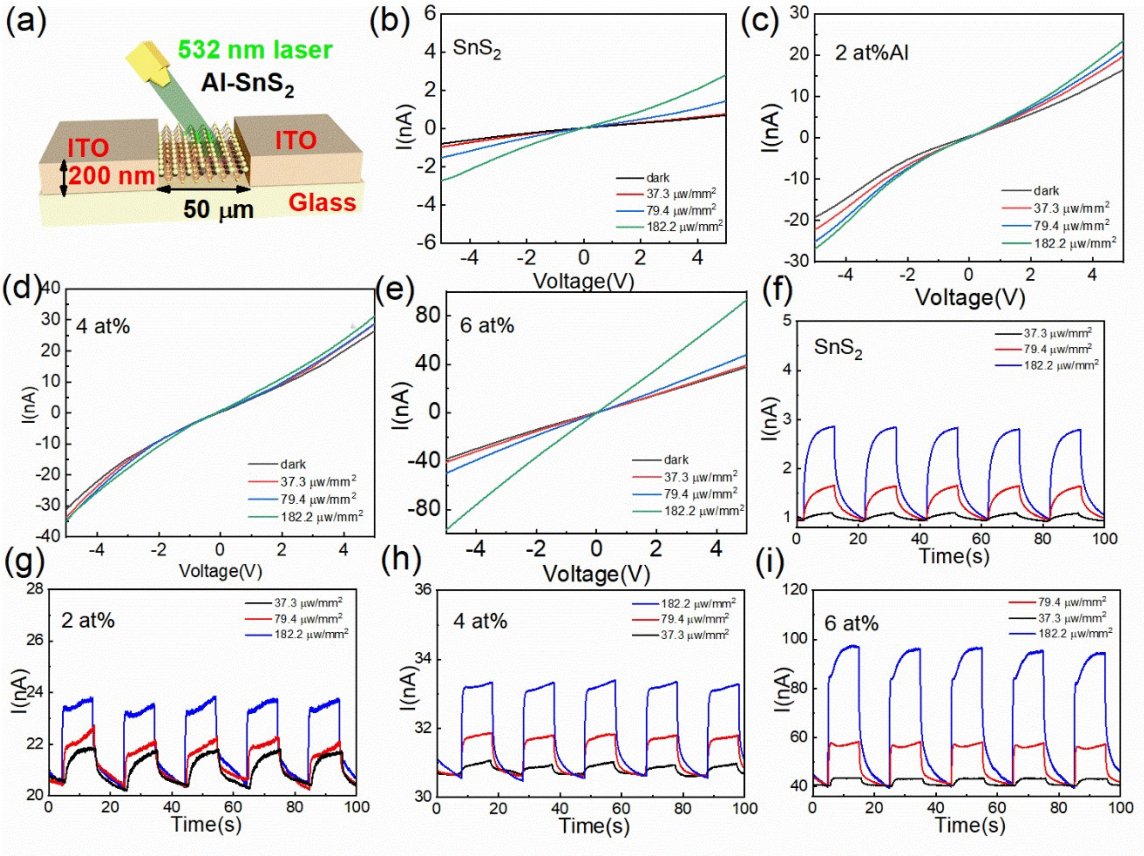

Figure S2. Photoresponse characterization for the pristine and Al-doped SnS_2 nanosheets. (a) Schematic diagram of a typical photodetector; Current-voltage(*I-V*) characteristics of (b) the pristine SnS_2, (c) 2 at%, (d) 4 at%, and (e) 6 at% Al-doped SnS_2 nanosheets under illumination of a 532-nm laser; Current-time (*I-T*) characteristics of (f) the pristine, (g) 2 at%, (h) 4 at%, and (i) 6 at% Al-doped SnS_2 nanosheets.

As shown in Figures. S2b-e, semilogarithmic current-voltage *I-V* curves for the pristine and Al-doped SnS_2 nanosheets show high symmetry, indicating ohmic contacts between the Al-doped SnS_2 nanosheets and ITO. Dark currents (I_{dark}) increased with increasing Al-doping concentration. Figures S2f-i show the current-time (*I-T*) characteristics for the pristine and Al-doped SnS_2 nanosheets under illumination by a 532-nm blue laser with different power densities. The chopping frequency was set as 50 mHz.

S-3 Comparison and analysis of the photoresponse characteristics under illumination of the 532-nm laser.

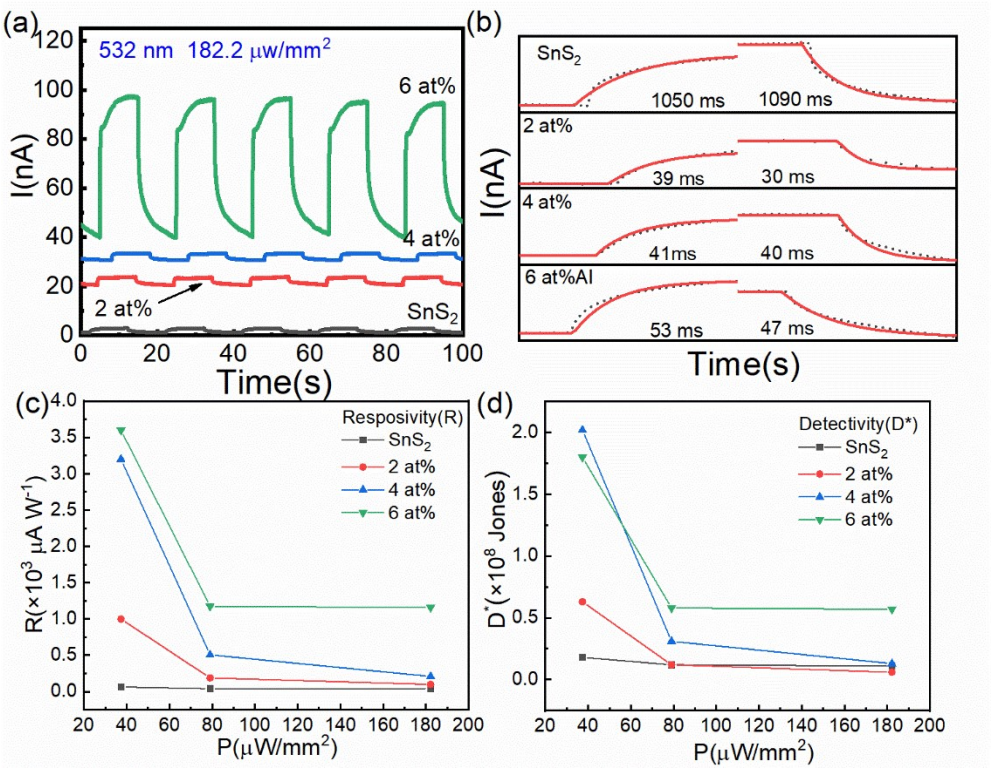

Figure S3. Comparison and analysis of the photoresponse characteristics under illumination of the 532-nm laser. (a) *I-T* curves for the pristine and Al-doped SnS_2 with different Al doping concentrations; (b) rise and fall times; (c) Responsivity and (d) Detectivity as a function of power density.

Figure S3a shows *I-T* curves of the photodetectors under illumination of a 532-nm laser with a power density of 182.2 μW/mm^2. The dark current of the photodetectors based on the Al-doped SnS_2 nanosheets were higher than that of the photodetector based on the pristine SnS_2 nanosheets. The response times of the Al-doped SnS_2 nanosheets, including the rise and fall times, were much less than that for the pristine SnS_2 as shown in Figure S3b. The photodetector of the 2 at% Al-doped SnS_2 nanosheets showed a fastest response to 50 mHz illumination. Figures S3c and d show the responsivity (R) and detectivity (D*) as a function of power density at the power density of 182.2 μW/cm^2. The responsivity and detectivity are 38.7 μA·W^{-1} and 1.1×10^6 for the pristine SnS_2 nanosheets, 99.1 μA·W^{-1} and 6.2×10^5 for the 2 at% Al-doped, 209.5 μA·W^{-1} and 1.3×10^6 for the 4 at% Al-doped SnS_2 nanosheets, 1160.3 μA·W^{-1} and 5.7×10^6 for the 6 at% Al-doped SnS_2 nanosheets.

S-4 Structural models of DFT calculations.

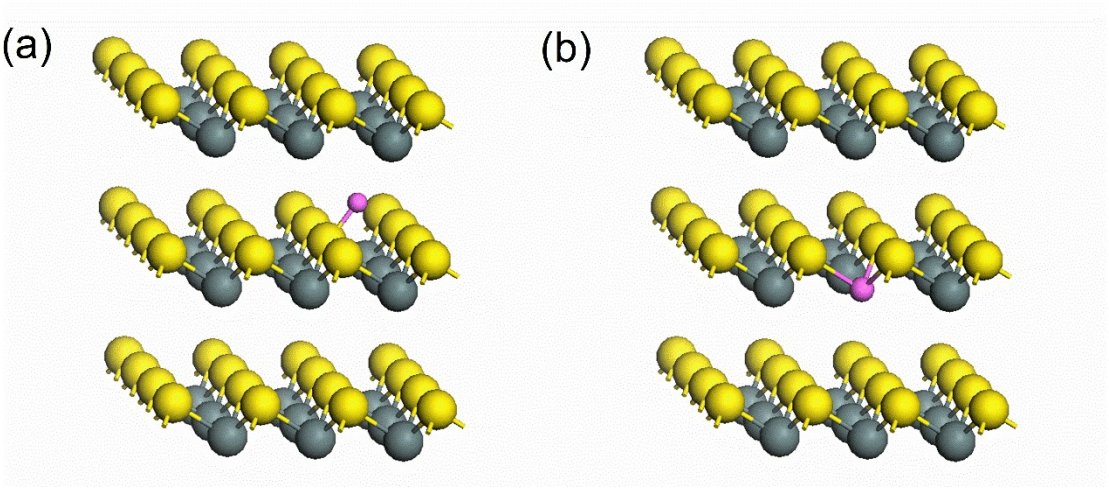

Figure S4. (a) Al intralayer intercalation; (b) Al substitution for Sn.

First-principles calculations are performed using the Vienna ab initio simulation package on basis of density-functional theory [1-2]. The exchange-correction interaction is treated by the generalized gradient approximation (GGA) with Perdew-Burke-Ernzerhof (PBE) functional. The valence electron configurations considered in this work are Al ($1s^2 2s^2 2p^6 3s^2 3p^1$), Sn ($4d^{10} 5s^2 5p^2$) and S ($3s^2 3p^4$), respectively. We simulate the Al-doped SnS_2 system by using the 3×3×3 repetition of a unit bulk SnS_2 cell as shown in Figure S4 a and b. The configurations of Al intralayer and substitution intercalation in the SnS_2 supercell are shown in Figures S5a-b. The cutoff energy is set to be 500 eV and the convergence accuracy of the self-consistent calculation is 10^{-5} eV. The Monkhorst-Pack grids of 3×3×3 was used for Brillouin zone integrations. All atoms in SnS_2 and Al-doped SnS_2 are fully relaxed until the components of residual forces are smaller than 0.05 eV/Å.

We have calculated the formation energy (E_f) by assuming the Sn and Al atom reservoirs are bulk Sn and bulk Al, thus $E_f = E_{doped} - E_0 - nE_{Al} + mE_{Sn}$, where E_{doped}, E_0, E_{Al} and E_{Sn} are the total energy of Al-doped SnS_2, pure SnS_2, bcc Al and fcc Sn, respectively. The integers n and m are the number of doped Al atoms and substituted Sn atoms, respectively. The calculated formation energies of substitutional and intralayer intercalated Aluminum defects are 5.31 and 4.46 eV, respectively. Thus, the substitution of Al can be easily generated than intralayer intercalation of In in SnS_2.

References:

[1] Kresse, G.; Hafner, J. Ab Initio Molecular Dynamics for Liquid Metals Phys. Rev.B 1993, 47, 558–561.

[2] Kresse, G.; Furthmüller, J. Efficient Iterative Schemes for Ab Initio Total-Energy Calculations Using a Plane-Wave Basis Set Phys. Rev. B 1996, 54, 11169–11186.